International Journal of Pharmaceutics 670 (2025) 125170

Contents lists available at ScienceDirect

International Journal of Pharmaceutics

journal homepage: www.elsevier.com/locate/ijpharm

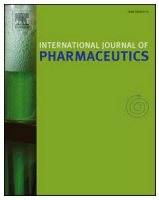

Supramolecular delivery systems for polyphenols: A green approach to predict *in vivo* permeability through an *in vitro* setup

Maddalena Sguizzato [a,*], Federica Agosta [a], Antonella Ciancetta [a], Mario Grassi [b], Rita Cortesi [a], Massimiliano Pio di Cagno [c,d]

[a] Department of Chemical, Pharmaceutical and Agricultural Sciences, University of Ferrara, Via Luigi Borsari, 46, 44121 Ferrara, Italy
[b] Department of Engineering and Architecture, University of Trieste, Via Alfonso Valerio, 6/1, 34127 Trieste, Italy
[c] Department of Chemical and Pharmaceutical Sciences, University of Trieste, Via Alfonso Valerio, 6/1, 34127 Trieste, Italy
[d] Department of Pharmacy, Faculty of Mathematics and Natural Sciences, University of Oslo, Sem Saelands vei 3, 0371 Oslo, Norway

ARTICLE INFO

Keywords:
Polyphenols
Natural molecules
Cyclodextrins
Inclusion complexes
Computational modelling
Permeability
Diffusivity
PermeaPad®

ABSTRACT

The use of *in vitro* markers able to reproduce the *in vivo* permeability and diffusivity of orally administered drugs, could represent an innovative starting point for the formulation of delivery systems, in particular for low soluble and low permeable drugs belonging to BCS class II and IV. Considering the great interest in the green pharmaceutical approaches and the increasing use of natural molecules as novel therapeutic drugs, in this study, rutin, hesperidin and curcumin have been selected as lipophilic model drugs to investigate their possible enhancement of their permeability and bioavailability after oral administration. As the low solubility of the three drugs hinders their application, β-cyclodextrins (CD), amphiphilic natural moieties able to form stable inclusion complexes, have been considered to promote their solubilization. Notably, hydroxypropyl-β-CD (HPBCD) and methyl-β-CD (MBCD), have been selected and the formation of the inclusion complexes with a stoichiometric ratio of 1:1 has been detected through phase-solubility studies and rationalized via docking calculations, revealing a strong complexation and an increased hydrophilicity of the systems. The diffusion experiments performed through the novel UV–Vis localized spectroscopy method confirmed a the extremely high stability of the CD-drugs complexes, especially in the cease of curcumin, which makes this as the predominant chemical specie to diffuse and permeates. The PermeaPad® plate, an *in vitro* cell-free assay, allowed to investigate the permeability behavior of the drugs, demonstrated that the type of β-cyclodextrins can influence the permeability through the biomimetic membrane, reflecting the effect of the unstirred water layer (UWL). Moreover, in the case of curcumin, the spectroscopic-mathematical approach suggested the formation of nano-supramolecular systems, detected by DLS, supporting the precision of the fitting model.

1. Introduction

The number of drugs (intended as active pharmaceutical ingredient, API) which exhibit poor biopharmaceutic profiles, *i.e.*, poor aqueous solubility and/or low permeability has steadily increased in the last years. Currently, BCS class II and IV drugs, *i.e.*, with poor aqueous solubility represents approx. 70 % of the product portfolio of the ten largest pharmaceutical companies (Jacobsen et al., 2023).

Poor thermodynamic aqueous solubility is generally attributed to the hydrophobic nature of the compound, *i.e.*, high partition coefficient (LogP), and/or to the high stability of the crystal lattice of the compound at the solid state which limits its dissolution (Bergström et al., 2016). These two different properties of drugs are colloquially referred to "grease ball" and "brick-dust" respectively. One of the oldest formulative strategy to enhance the apparent solubility of "grease ball" as well as "brick-dust" compounds has been the solubilization with

Abbreviations: BCS, Biopharmaceutics Classification System; CD, cyclodextrin; HPBCD, hydroxypropyl-β-cyclodextrin; MBCD, methyl-β-cyclodextrin; UWL, unstirred water layers; RU, rutin; HES, hesperidin; CUR, curcumin; PBS, Phosphate-buffered saline; C_C, concentration of inclusion complex; C_D, concentration of free drug; J_C, flux of inclusion complex; J_D, flux of the free drug; J_{app}, apparent flux measured *in vitro*; P_C, permeability of inclusion complex through the biomimetic barrier; P_D, permeability of free drug through the biomimetic barrier; P_{app}, apparent permeability; D_C, diffusivity of inclusion complex; D_D, diffusivity of free drug; C_N, nominal concentration; C_0, concentration from fitting..

* Corresponding author.
E-mail address: sgzmdl@unife.it (M. Sguizzato).

https://doi.org/10.1016/j.ijpharm.2025.125170
Received 17 September 2024; Received in revised form 2 January 2025; Accepted 2 January 2025
Available online 3 January 2025

amphiphilic moieties such as cyclodextrins (CDs).

These cyclic oligosaccharides are composed of several glucose units joined by α-1,4 glycosidic bonds (Fig. 1). Among cyclodextrins, cycled macromolecules consisting of 6 (α-CD), 7 (β-CD) and 8 (γ-CD) glucose units (Loftsson and Brewster, 2010) (Fig. 1), the most employed for pharmaceutical purposes is β-CD and its hydrophilic derivatives, namely hydroxypropyl-β-CD (HPBCD) and methyl-β-CD (MBCD) (Fig. 1). β-CDs are capable of creating spontaneous complexes in water with small/medium drug molecules, whereby the ligand (L), by including its lipophilic portion, most commonly aromatic/benzyl rings, into their hydrophobic core, forms stable inclusion complexes of higher water solubility with respect to native drug (Fig. 1) (Di Cagno, 2016). The stability of the CD-L complex is evaluated through its equilibrium constant (K, Fig. 1), which is often (but not always) stoichiometrically a 1:1 complexation ($K_{1:1}$, n = m in Fig. 1).

Notwithstanding the effective (or "apparent") increase of solubility in water of the complexed lipophilic drugs, it is still unclear whether utilization of CD is beneficial for orally administered formulations to improve bioavailability of carried lipophilic drug. Carrier at al. (Carrier et al., 2007) reported a list of 24 active ingredients where the utilization of some type of CDs resulted beneficial in terms of oral bioavailability *in vivo*. On the other hands, CDs were found to have a negative effect on overall drug absorption both *in vitro* (Sugano and Terada, 2015) as well as *in vivo* (Holm et al., 2016) with different drugs. It is generally accepted that the mechanism by which CD can increase oral bioavailability of a lipophilic API is based on increased dissolution rate of the solid dosage form (*i.e.*, tablet) followed by a "rapid" release of the drug from the CD cavity close to the absorption barrier. The diagram in Fig. 2 schematizes the mechanism of drug permeation *in vitro* for a CD formulation. In this accepted model, only the free drug fraction (*i.e.*, not loaded into the CD) permeates through the barrier (blue ovals in Fig. 2).

To the best of our knowledge, the possibility for the CD-L complex to be adsorbed has been explored on Caco-2 cell layers (Haimhoffer et al., 2019; Réti-Nagy et al., 2015), but it has never been investigated *in vitro* in a cell-free model setup. The aim of the present study was to find evidence supporting the permeation of CD-drug complex *in vitro* and the validity of the permeation model described in Fig. 2, in particular for poor soluble and poor permeable drugs. Tzanova et al. has recently provided solid *in vitro* indications that for at least two drugs, namely, ketoprofen and hydrocortisone, at very high solubilization, *i.e.*, very high apparent solubility (over 25 mM), permeation of the CD-drug complex (Fig. 2, yellow line) might occur *in vitro*, thus providing a higher net drug absorption.

The diagram of Fig. 2 describes the situation at equilibrium, *i.e.*, in steady state flux conditions and it fit well for lipophilic compound (*i.e.*, positive LogP) with intermediate permeability. The premises of this model are that the free drug and the CD-drug complex must be considered as two different chemical species which diffuse spontaneously through unstirred water layers (UWL) and a biomimetic barrier. At the equilibrium, the free drug (blue ovals) has a much lower concentration (C_D) than the CD-drug complex (C_C), generating a much lower concentration gradient. However, this is compensated by a sufficiently high permeability (P_D) through the barrier and diffusivity (D_D) in the unstirred water layer (UWL). On the other hand, and despite the very high concentration gradient generated by the CD solubilization (C_C), the CD-drug complex will have a much lower permeability (P_C) through the barrier and diffusivity in the UWL (P_C). Assuming equal thickness for the UWL in the acceptor and donor compartment (h), and equal permeation area, the apparent flux measured *in vitro* (J_{app}), could be described as the sum of the flux of the free drug (J_D) and the flux of the CD-drug complex (J_{CD}) (Eq. (1) and Fig. 1).

$$J_{app} = J_D + J_C = \left(\frac{D_D P_D}{2hP_D + D_D}\right)^* C_D + \left(\frac{D_C P_C}{2hP_C + D_C}\right)^* C_C \quad (1)$$

where D_D and D_C indicate the diffusion coefficient of the free drug and CD-drug complex respectively, and P_D and P_C the net permeabilities of the free drug and the CD-drug complex.

According to this model, in the case of *i.* a highly stable CD-drug complex where *ii.* the concentration of the CD-drug complex is significantly higher than the free drug concentration ($C_{CD} \gg\gg C_D$ and $\approx C_{tot}$) and *iii.* the permeability of the free drug is comparable to the permeability of the complex drug-CD ($P_D \approx P_C$), the net flux should be attributed solely to the CD-drug complex (Eq. (2).

$$J_{app} \approx \left(\frac{D_C P_C}{2hP_C + D_C}\right)^* C_C \quad (2)$$

Having on eye on green transition, we employed three natural products which are known to have extremely poor permeability *i.e.*, rutin, hesperidin, and curcumin (Table 1) selected as model drugs. In the present study we investigated the complexation properties of the selected compounds, with two different types of cyclodextrins (*i.e.*, HPBCD and MBCD) and applied computational modelling to investigate the mechanism as well as the stoichiometry of the complexation. We characterized the concentration of the free drug (L) and the diffusivities

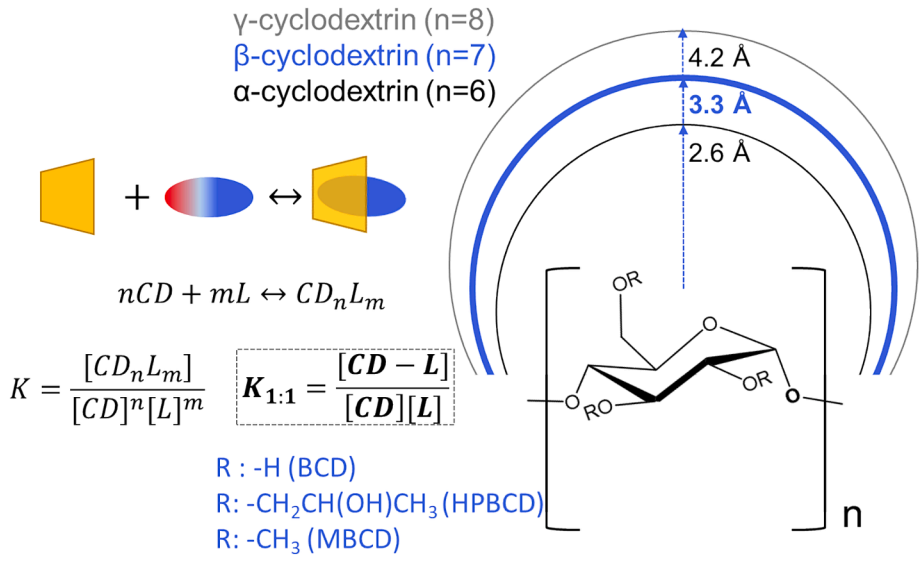

Fig. 1. General structure, geometrical characteristics, and schematic representation of the formation of a cyclodextrin (CD) inclusion complex most commonly used in pharmaceutics with a ligand (L). $K_{1:1}$ represent the stability constant (K) in case of a 1:1 stoichiometry reaction (*i.e.*, n = m = 1).

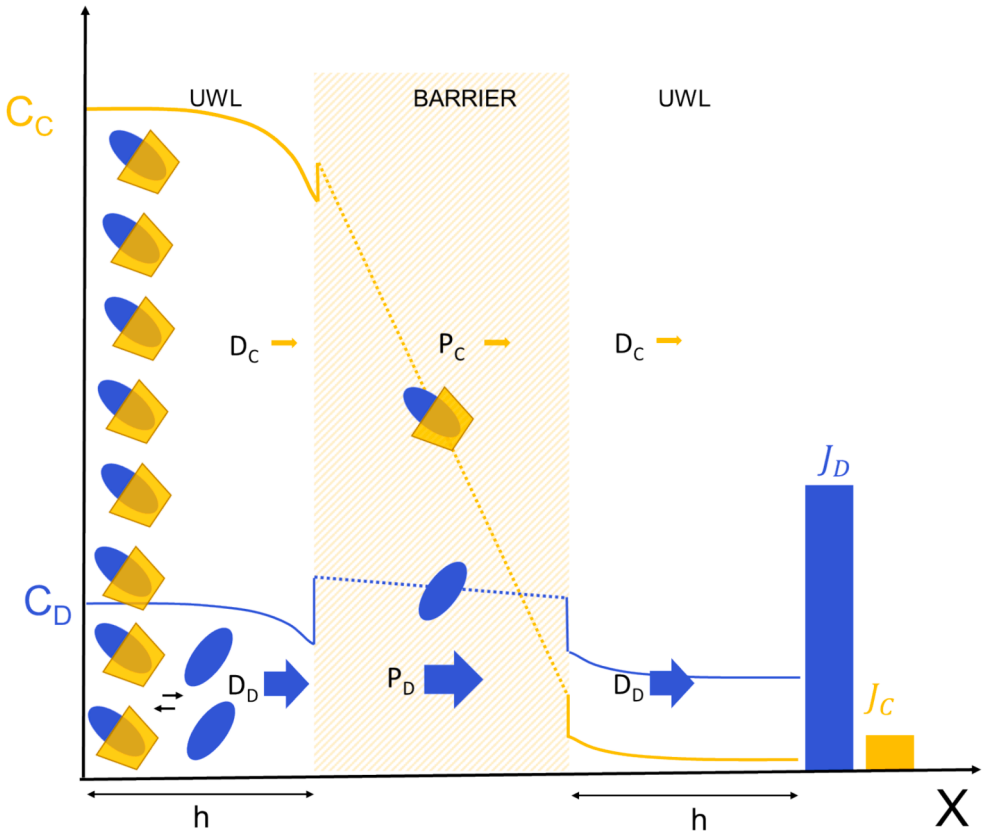

Fig. 2. Physical model describing the permeation of a drug *in vitro* in the presence of cyclodextrins. Even though the CD-drug complex has a much higher concentration (C_C), in comparison to the free drug (C_D), the flux of the free drug (J_D) is predominant in comparison to CD-drug complex (J_C) form medium permeable compounds. In this model the free drug and CD-drug complex are treated as different chemical species, with different diffusivities through the unstirred water layer, UWL (D_D and D_C respectively) as well with different permeabilities through the biomimetic barrier (P_D and P_C respectively).

Table 1
General characteristics of the selected drugs: chemical structure and physicochemical properties (MW, molecular weight; λ_{max} , wavelength of maximum absorbance; LogP, partition coefficient octanol–water) reported in literature (source PubChem).

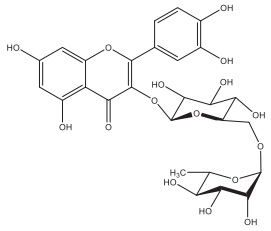	RUTIN. 3′,4′,5,7-Tetrahydroxy-3-[α-L rhamnopyranosyl- (1 → 6)-β-D-glucopyranosyloxy]flavone	MW: 610.52 g/mol λ_{max}: 360 nm LogP: −1.3
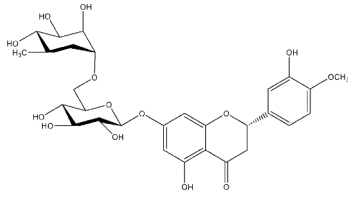	HESPERIDIN. (2S)-3′,5-Dihydroxy-4′-methoxy-7-[α-L-rhamnopyranosyl (1 → 6)-β-D-glucopyranosyloxy]flavan-4-one	MW: 610.60 g/mol λ_{max}: 283 nm LogP: −1.1
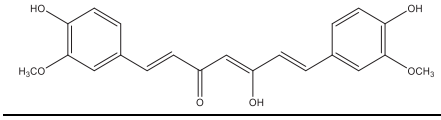	CURCUMIN. (1E,6E)-1,7-Bis(4-hydroxy-3-methoxyphenyl) hepta-1,6-diene-3,5-dione	MW: 368.38 g/mol λ_{max}: 425 nm LogP: 3.2

of both species involved in the permeation, *i.e.*, free drug and CD-drug complex by UV–vis localized spectroscopy/mathematical data fitting (Tzanova et al., 2022), during diffusion and we measured the *in vitro* permeability of these formulations through the state-of-the-art PermeaPad® multiwell plates. Hence, the main focus is to exploit a simple delivery strategy to enhance solubility of poor soluble and poor permeable drugs and translate the theoretical diffusion data and better understand the permeability process of the investigated compounds, to find evidence that the diffusion of the drugs is governed by the free or the complexed form.

2. Materials and Methods

2.1. Materials

Hydroxypropyl-β-cyclodextrin (HPBCD), methyl-β-cyclodextrin (MBCD), rutin (3,3′,4′,5,7-Pentahydroxyflavone 3-rutinoside, RU), hesperidin (3′,5,7-Trihydroxy 4′-methoxyflavanone 7-rutinoside, HES), curcumin ((E,E)-1,7-bis(4-Hydroxy-3-methoxyphenyl)-1,6-heptadiene-3,5-dione, CUR), and ethanol (EtOH) were purchased from Merck. All solutions were prepared with water purified by a Milli-Q® water purification system for ultrapure water by Merk Millipore (Darmstadt, DE). Phosphate-buffered saline (PBS, 73 mM) solutions with pH 7.4 was prepared as follows: one part 2.5 % (w/v) $NaH_2PO_4{\cdot}2H_2O$ solution was mixed with four parts 0.9 % (w/v) $Na_2HPO_4{\cdot}2H_2O$ solution. The pH was adjusted to 7.4 ± 0.05 (SevenCompactTM pH/ion metre S220; Mettler Toledo, Columbus, OH, USA) with NaOH pellets. The osmolality was adjusted to 280 − 300 mOsm/ kg (Semi-Micro Osmometer K-7400, Knauer, Berlin, DE) with NaCl, and the solution was filtered 0.2 μm (Whatman® Nuclepore Track-Etch membrane filter; GE Healthcare Life Sciences, Maidstone, UK) before use (Tzanova et al., 2023).

2.2. Phase-solubility studies

Cyclodextrin (CD) solutions were prepared with increasing concentrations of HPBCD and MBCD as follow: 0 (only solution), 5, 10, 20, 50 mM. They were incubated overnight protected by light with RU, HES and CUR to reach saturated solutions. Then, the solutions were filtered through a 0.2 μm PES syringe filter (VWR International, Radnor, PA, USA) and diluted for the quantification by UV/Vis spectrophotometer (λ_{max} 360 nm, 283 nm, 425 nm for RU, HES, CUR, respectively). The drug concentration of each CD-drug complex was plotted as a function of CD concentration and the binding constant $K_{1:1}$ (M^{-1}) was calculated as reported in Eq. (3):

$$K1{:}1 = \frac{slope}{C_0(1 - slope)} \tag{3}$$

where slope is determined from the diagram according to Higuchi and Connors' model and C_0 is the thermodynamic solubility of each compound in PBS.

2.3. Molecular docking

Molecular Docking calculations were performed using the Autodock-Vina software (Morris et al., 2009).

The three-dimensional structure of the MBCD was extracted from the Protein Data Bank (Berman, 2000) (PDB ID: 6XX3) (Plaza-Garrido et al., 2020), while the structure of the HPBCD was constructed by manually attaching the isopropyl groups on the glucopyranose 6-OH group (PDB ID: 3CGT) (Schmidt et al., 1998). The HPBCD geometry was optimized using the *quickprep* module as implemented in MOE (Molecular Operating Environment (MOE), 2022) to check for the compound protonation state and minimize the initial coordinates. Ligand structures were retrieved from PubChem (Kim et al., 2023).

Protein and ligand structure preparation for docking was performed using Autodock Tools python scripts (Morris et al., 2009), by adding polar hydrogen atoms, computing Gasteiger charges, and assigning AD4 atom types. The grid box dimensions were set as 15 Å x 15 Å x 15 Å, while the center was defined by using the "centerofmass" function in Pymol: 58.171 (x); 12.140 (y); 9.136 (z) and −8.173 (x); 14.267 (y); 14.000 (z) for HPBCD and MBCD, respectively. Output files were analysed and clustered in PyMOL (Schrödinger and DeLano, 2021) while LogP values of the ligand and CD complexed were computed with MOE (Molecular Operating Environment (MOE), 2022).

2.4. Diffusion studies

Localized UV–Vis spectroscopy measurements were performed on a double array UV–Vis spectrophotometer UV-6300PC (VWR International, Radnor, PA, USA) in semi-micro cuvettes with PTFE stopper (Vchamber = 700 μL, path length = 10 mm; Starna Scientific®, Essex, UK), as previously described (Di Cagno et al., 2018). The diffusion medium and reference sample (675 μL each) consisted of Milli-Q®, whilst the donor solution contained drug solutions or CD-drug complexes (CD concentration of 10 mM). At time zero (t = 0 s), donor solution (25 μL) was injected at the bottom of the sample cuvette using a microneedle syringe (Hamilton Company, Reno, NV, USA). Absorbance measurements were recorded at 360 nm, 283 nm, 425 nm for RU, HES and CUR, respectively, every 120 s for a total of 24 h. For all experiments, the sample cuvette was lifted by 0.60 cm using a 3D-printed stand, in order to re-cord absorbances at precisely 0.51 cm (detection position, XD) from the bottom of the cuvette (*i.e.* the origin of diffusion), as previously reported (Di Cagno et al., 2018). The experimental diffusion profiles data were fitted through mathematical modelling to a numerical solution of Fick's diffusion law (Eq. (1) in order to extract the diffusivity (D) and drug concentration (C) as described in Tzanova et al. (Tzanova et al., 2022).

$$\frac{\partial C}{\partial t} = \left(\frac{\partial}{\partial x}\left(D\frac{\partial C}{\partial x}\right)\right) \tag{4}$$

2.5. Permeability studies with PermeaPad® plate

Reference permeability of the drug (P_D, *i.e.*, in PBS) of RU, HES, CUR in PBS and apparent permeability (P_{app}, *i.e.*, in presence of HPBCD and MBCD 5 mM) was investigated using 96-well PermeaPad® plate (Phabioc GmbH, Espelkamp, DE), constituted of an artificial biomimetic barrier. The acceptor phase consisted of PBS pH 7.4 (400 μl) for all conditions, while in the donor phase 200 μl of drug solution in PBS or HPBCD- and MBCD-drug complex were loaded. The plate was incubated in an orbital shaker-incubator (ES-20, Biosan, Riga, LV) at 25 °C for 8 h and shaken at 200 rpm. At the end, 100 μl of sample were withdrawn from the acceptor compartment and drug concentrations were determined by spectrophotometric analysis on a Spectramax 190 Microplate Reader (Molecular Devices Inc., Sunnyvale, CA, USA) at drug-specific wavelengths reported above. Standard solutions for each drug were measured on the same plate, and PBS absorbance was subtracted from all measurements. Fluxes (J) were calculated with Eq. (5a):

$$J = \frac{Q_t}{A} * \frac{1}{t} \tag{5a}$$

$$P_D = \frac{J}{S_0} \tag{5b}$$

dividing the amount of drug permeated through the barrier at the end of the incubation (Q_t) by the area of the membrane (A, 0.13 cm^2) and the time of incubation (t). For the drug solution (*i.e.,* with no CD), the reference apparent permeability for the drug (P_D) was calculated by Eq. (5b), *i.e.*, by normalizing the measured flux over the drug thermodynamic solubility measured (S_0).

2.6. Size analysis

The intensity-mean hydrodynamic diameter (z-average (nm)) was measured using dynamic light scattering (DLS) with a red-light laser (λ = 633 nm) at 25 °C by Zetasizer Nano-ZS (Malvern Instruments, Oxford, UK). The refractive index and the viscosity of pure water at 25 °C were used as constant parameters in the calculations. The analysis (300 s, 3 cycles, 25°C) was performed on CD-drug complexes samples in disposable polystyrene cuvette for Zetasizer (Sarstedt AG & Co., Nümbrecht, DE).

3. Results and Discussions

There is a growing interest in predictive markers able to simulate the *in vivo* permeability and diffusivity in an *in vitro/in-silico* setup, in particular for natural drugs involved in the 3Rs concept, supporting an ecological consciousness and awareness. Among this category, RU, HES and CUR represent good candidates for the investigation developed in this work. Indeed, they possess multiple therapeutic activities (Chua, 2013; Grasso et al., 2021; Hao et al., 2023; Mukherjee and Krishnan, 2023; Negahdari et al., 2021; Pyrzynska, 2022; Santa et al., 2023; Servida et al., 2024; Xiong et al., 2019) hindered by low bioavailability, limited dissolution rate and limited stability. Hence, considering the complexation strategies previously reported for different applications (Gözcü et al., 2024; Paczkowska et al., 2015; Song et al., 2023), the use of CDs as a tool to increase the aqueous solubility has been considered, with the aim of shedding light on their permeation and diffusion in their free or bound form. Notwithstanding, the use of a spectroscopic method coupled with the mathematical fitting as a tool to clarify the permeation model of extremely poor soluble molecules in the form of free drug or CD-drug complex has not been demonstrated.

3.1. Molecular modelling

The complexation of the drugs with HPBCD or MBCD was investigated *in silico* to elucidate the influence of the CD type. The analysis of CD inclusion complexes was carried out by assuming a drug-CD stoichiometric ratio of 1:1, and docking poses of RU, HES and CUR in complex with HPBCD and MBCD are shown in Fig. 3.

As displayed, RU and HES are included in the CD cavity by the flavonoid motif, with a different orientation of the glucoside portion, whereas CUR presents a "bent conformation". In particular, the insertion of the A ring of RU into the CD cavity could be responsible for its supramolecular interactions with the CD. As far as HES is concerned, for both CD types, the glucoside region protrudes out of the cavity in all poses (up or down and opposite to the ring C). In the case of CUR, the "bent conformation" could be responsible for a reduced entropic contribution in the CD complex formation and in particular with HPBCD, whereas in the CUR-MBCD complex, the drug is partially exposed to the solvent. These data corroborate the results reported in literature, confirming the complexation with CD in a stoichiometry ratio 1:1 (Chang et al., 2023; Song et al., 2023; Wdowiak et al., 2022). Furthermore, the physicochemical properties of the complexes have been calculated in MOE and the results of LogP estimated ($LogP_C$) referred to the free drug and the CD-complexes are reported in Table 2. The computational model supports for all compounds the assumed 1:1 stoichiometry.

Concerning the $LogP_C$ of free drugs, the data confirmed the values reported in literature, previously summarized in Table 1. Moreover, the calculated $LogP_C$ values of CD-drug complexes confirmed that the complexation allowed to enhance the solubilization of the molecules and, as a consequence, their hydrophilicity. In all cases, the $LogP_C$ of drug-HPBCD and drug-MBCD resulted in a 5 to 4-fold decrease, even passing from a positive to a negative value for CUR. Considering the low solubility of the drugs in PBS, namely S_0 (Table 2), the calculated $LogP_C$ are in agreement with them.

3.2. Phase-solubility studies

The stoichiometry of complexation was clarified by molecular modelling, and the phase-solubility studies were performed following the classical approach introduced by Higuchi and Connors (Higuchi and Connors, 1965), allowing to calculate the equilibrium constants of the CD-drug complex as reported in Eq. (3), and the results are shown in Fig. 4.

Table 2
Experimental and predicted physicochemical properties of the investigated drugs (ε, molar extinction coefficient; S_0 , measured solubility of drug in PBS pH 7.4; $LogP_C$, partition coefficient octanol–water calculated with MOE; P_D , drug reference permeability measured from PermeaPad® plate permeability experiments).

Drug	ε (cm^2/mmol)	S_0 (μg/ml)	$LogP_C$	$LogP_C$ drug-HPBCD	$LogP_C$ drug-MBCD	P_D (cm/s)
RUTIN	14.24	61.7	−1.02	−5.11	−5.11	2.22×10^{-6}
HESPERIDIN	18.95	7.7	−1.01	−4.25	−4.25	2.80×10^{-6}
CURCUMIN	4.66	*0.3	3.74	−0.38	−0.38	*4.24×10^{-7}

* in PBS/EtOH 0.5%.

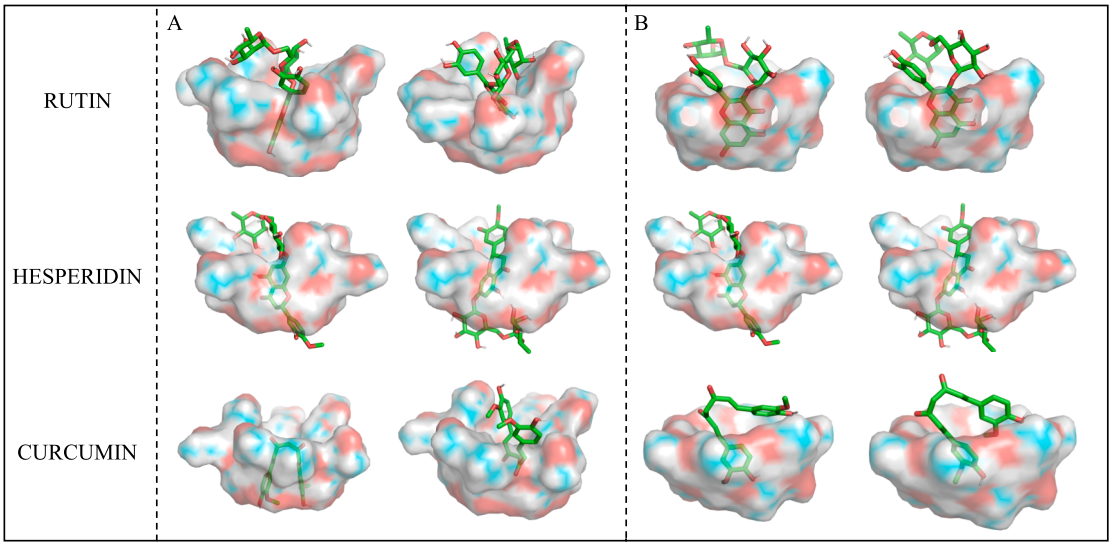

Fig. 3. Docking poses of cyclodextrin inclusion complexes. For each compound in complex with both HPBCD (A) and MBCD (B), two clusters (left and right panels), differing for the orientation and placement of the glucoside region, were identified. Ligand structures are shown as sticks color coded by atom type with green carbon atoms while CD structures as surfaces color coded by atom type with cyan carbon atoms, respectively. (For interpretation of the references to color in this figure legend, the reader is referred to the web version of this article.)

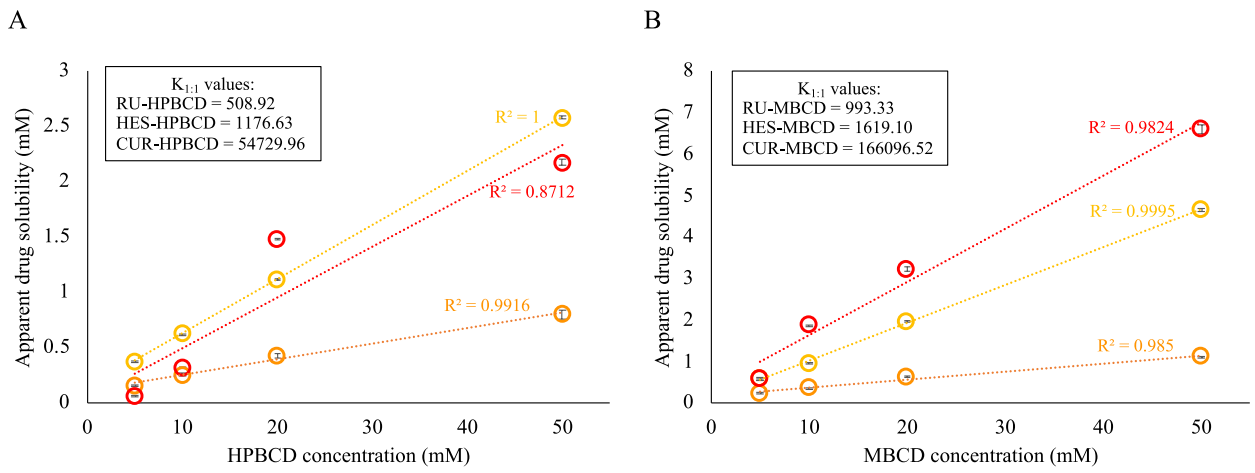

Fig. 4. Phase-solubility studies of RU (yellow), HES (orange) and CUR (red) with increasing concentrations of HPBCD (panel A) and MBCD (panel B). Binding constants ($K_{1:1}$) of the drugs to HPBCD and MBCD are reported in the upper panels. Data are the average of three measurements ± s.d. (For interpretation of the references to color in this figure legend, the reader is referred to the web version of this article.)

The phase-solubility diagrams revealed an A_L type behavior, in agreement with the 1:1 stoichiometry of the inclusion complex supported by the computational model (Fig. 1). The results demonstrated a linear regression of the increased drugs concentration, as evidenced by R^2 values: the higher the CD concentration, the higher the apparent drug solubility. In the case of CUR-HPBCD, a lower R^2 value of linear fitting was acquired, most likely due to the possible formation of aggregates of the CD-CUR complex at the higher HPBCD concentrations. Nevertheless, the obtained results are consistent and is in accordance with literature, where different β-CDs were a 1:1 stoichiometry is reported for β-CDs-CUR complexation (Jiang et al., 2022; Mashaqbeh et al., 2021; Saokham et al., 2018; Song et al., 2023; Yadav et al., 2009).

In general, the complexation with MBCD determined the greatest apparent solubility for all selected drugs, thus suggesting that the best CD-drug complex is reached, in terms of solubility and stability. This observation is also confirmed by the larger values of binding constants ($K_{1:1}$) reported for MBCD (Fig. 4B) with respect to HPBCD (Fig. 4A). As previously underlined, this result was particularly evident for CUR, where the apparent solubility with the maximum concentration of MBCD was 3-fold higher with respect to those with HPBCD. This behavior could be ascribed to a change in the drug binding conformation in the CD as suggested by molecular docking (Fig. 3).

Finally, RU, HES and CUR possess a different grade of hydrophilicity, as expressed by their aqueous solubility (S_0, Table 2), and for higher S_0 values, the lowest equilibrium constants were measured, as reported in the upper panels of Fig. 4.

3.3. *Diffusion studies by UV–vis localized spectroscopy/mathematical data fitting*

The open question of the present investigation is the possibility for the CD-drug complexes to be sufficiently stable to be absorbed as one chemical entity. With this aim, the diffusion of the free drugs and the CD-drug complexes was evaluated *in vitro* using UV–vis localized spectroscopy coupled with mathematical data fitting (Di Cagno et al., 2018; Tzanova et al., 2023).

The evaluation of the diffusion coefficient is a crucial point to predict the absorption of a drug, and in the pharmaceutical development represents an essential parameter to predict its bioavailability. In addition, the coupled method used in this study allows the extraction not only of the diffusion coefficients of the investigated species, but also the drug concentrations (C_0) to be compared with the nominal ones (C_N). Hence, the comparison between C_0 and C_N allows to validate the influence of the free drug on the diffusion with respect to the complexed form. Table 3 reports the complete summary of all data-fitting.

In this case, giving the significantly higher concentration of the drug-CD species over the free drug species obtained by solubilizations, it is acceptable to assume that the diffusivity corresponds to be the diffusivity of the Drug-CD complex (D_C). In the case of RU drug solution (*i.e.,* no CD), the concentration from fitting, *i.e.,* C_0, was superimposable to C_N. The same result was found for the CD dispersions for RU, but as in this case C_N refers to the apparent solubilization generated by the cyclodextrin (CD-L concentration) it is safe to state that the CD-RU is very stable and remains stable over the diffusion. Additionally, comparing the measured diffusivity (D_C) of the free drug with those of

Table 3
Fitting parameters referring to drug in PBS and complexed with 10 mM HPBCD and MBCD obtained by diffusion studies (h, detection point, distance from the origin of diffusion, *i.e.*, bottom of the cuvette; C_N , nominal concentration; C_0 , concentration from fitting; D_C , mean diffusivity.

Drug name	h cm	V injected µL	V acceptor µL	C_N µg/mL	C_0 µg/mL	ΔC %	CD type	CD conc mM	D_C cm^2/sec	K_p	Error X2
RU	0.51	25	675	61.4	62.7	2	–	0	4.18×10^{-6}	1	0.85
RU	0.51	25	675	382.0	328.7	−14	HPBCD	10	3.20×10^{-6}	1	50.98
RU	0.51	25	675	595.9	533.0	−11	MBCD	10	2.88×10^{-6}	1	137.48
HES	0.51	25	675	11.0	15.8	44	–	0	4.22×10^{-6}	1	0.10
HES	0.51	25	675	156.5	171.8	10	HPBCD	10	2.52×10^{-6}	1	17.82
HES	0.51	25	675	228.6	272.2	19	MBCD	10	2.73×10^{-6}	1	110.47
CUR	0.51	25	675				–	0	*4.87×10^{-6}*	*1*	*Estimated*
CUR	0.51	25	675	118.5	55.0	−54	HPBCD	10	2.76×10^{-6}	1	0.91
CUR	0.51	25	675	693.2	317.3	−54	MBCD	10	2.51×10^{-6}	1	42.06

the RU-HPBCD and RU-MBCD, the higher value of the free form confirms that the contribution of the free drug in the net mass diffusion process is irrelevant. Hence, this result suggests that the diffusivity is governed by the CD complexes.

For HES, the diffusion parameters revealed a similar behavior to RU, corroborating the same statements. In particular, with HPBCD the profile clearly follows a Fickian diffusion, where the flux is concentration-dependent.

Regarding CUR, the results revealed similar trend but with a surprising discrepancy. Firstly, it has to be noticed that the diffusion of the sole CUR was estimated from its molecular weight due to the undetectable concentration of CUR in PBS. Then, concerning the diffusion of CUR-HPBCD, it seems to follow an almost perfect Fickian profile, where the experimental fitting is superimposable to the model one (Fig. A.1). This is an additional indication that the binding constant CUR-CD is very high and the complex very stable. The situation for the MBCD was quite similar and also in this case the experimental and the model fitting show the same pattern.

Surprisingly, for CUR, C_0 differed largely from C_N. Specifically, for both CDs resulted approximately half of C_N values in all conditions. These results are very relevant as they imply in practice that approximately half of the CUR in which is solubilized is actually not contributing to the concentration gradient, driving force of the diffusion and permeation processes, and therefore not directly available to diffusion as well as permeation. This observation is a clear indication of the formation of macromolecular aggregates CUR-CD (as previously observed by (Li et al., 2022).

To verify this hypothesis, DLS analysis of CD-drug complexes were performed. No evidence of aggregates was detected in the case of RU-CD and HES-CD. On the other hand, in the case of CUR-HPBCD and CUR-MBCD different populations of around 211.4 ± 36.9 nm and 116.9 ± 79.8 nm, respectively, were detected (Fig. A.2). This result demonstrated that CUR-CD complexes generate colloidal species, *e.g.* nano-supramolecular systems, which are rather stable in aqueous dispersion but, at the same time, they are responsible for the lower availability for diffusion, as similarly reported in literature (Li et al., 2022; Wankar et al., 2020; Wei et al., 2015).

3.4. Permeability studies with PermeaPad® plate

Besides the evaluation of the diffusion coefficients for RU, HES, CUR in free and complexed form, the permeability was also investigated for a complete prediction of drug uptake and bioavailability.

Permeability experiments were performed on free drugs (namely P_D) and CD-drug complexes with the PermeaPad® Plate, a state-of-the-art *in vitro* cell-free assay. This biomimetic phospholipid-based membrane is mounted in a 96-wells plate by separating the lower and upper compartments and an unstirred water layer (UWL) on each side of the membrane. Thus, the barrier consists of three distinct regions and a concentration gradient within and between each layer (Eriksen et al., 2022), leading to significantly increasing the throughput of permeability experiments, with respect to other type cell-free permeation tool, such as PAMPA barriers (Jacobsen et al., 2020; Morita et al., 2024). Additionally, the use of PermeaPad® membranes has never been considered to investigate the permeability behavior of the selected drugs, and the following results can elucidate for the first time the influence of this type of membrane on their permeability.

The reference permeability for each drug (P_D, Table 2) was low-very low, ranging in the order of magnitude from 10^{-6} cm/sec for RU and HES to 10^{-7} cm/sec for CUR. Due to the extremely low solubility of CUR in water, the permeability experiments for the pure drug were performed in PBS/ethanol 0.5 % solutions, as the addition of a small aliquot of ethanol in the donor solution was necessary to allow the solubilization of CUR and to evaluate the permeability behavior. The results are in accordance with the physicochemical properties of the compounds and with their BCS classification (Dahan et al., 2009). In fact, the selected compounds are classified as poor permeable and/or soluble drugs, belonging to class II (RU) and class IV (HES and CUR), thus confirming the data reported in literature (Shekaari et al., 2023; Wahlang et al., 2011; Yusuf et al., 2023).

The influence of the CD on drug permeability has been investigated and, considering Fick's law involvement in passive drug diffusion, the changes in the apparent flux (*i.e.*, the rate of the drug passage through the membrane) have been evaluated. The results of the experiment, expressed as flux variation of drug permeated through the membrane, are reported in Fig. 5.

Comparing the apparent fluxes generated by the CD-drug complexes with those of the free drugs, the calculated variation was significant, thus indicating that the type of CD can influence the drug permeability.

In details, for RU, apparent fluxes generated by RU-HPBCD and RU-MBCD slightly changed (0.80 and 0.82, respectively) suggesting that both the free drug and the CD-RU complex could permeate through the membrane. In the same way, the slight reduction in permeability obtained with the complexed forms is in accordance with the extrapolated diffusivity (D_C) values obtained with the mathematical fitting (Table 3), where the contribution of the complexed drug was detected.

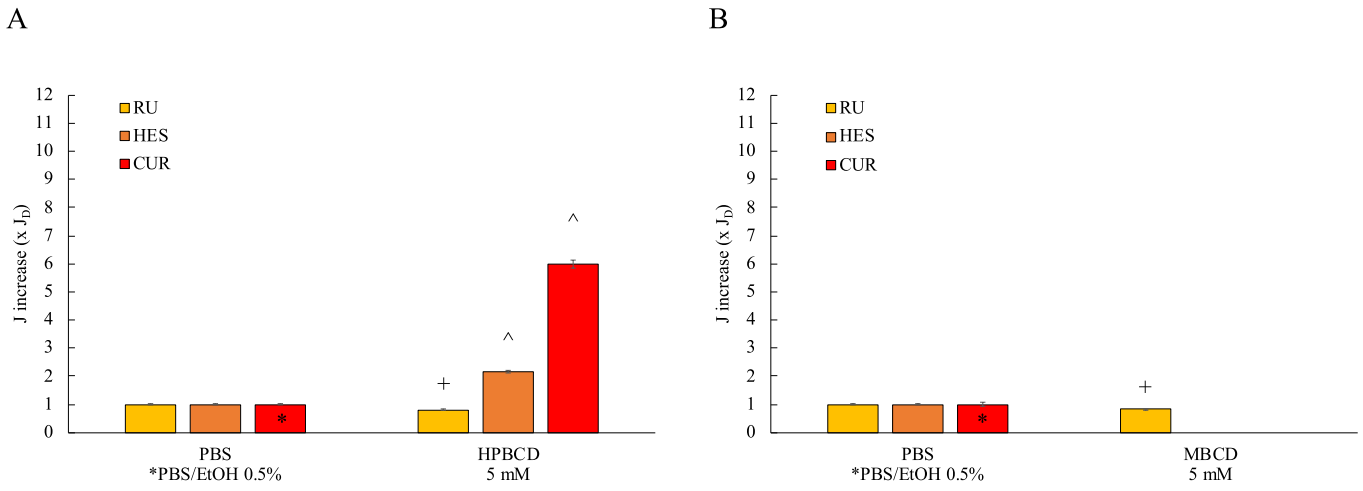

Fig. 5. Flux variation of RU (yellow), HES (orange) and CUR (red) through biomimetic PermeaPad® from drug solution and HPBCD complex (panel A) or MBCD complex (panel B). Data are normalized with respect to the flux of the free drug (J_D) measured over 4 h incubation. Data are the average of three measurements ± SD *PBS/EtOH 0.5 %; + $p < 0.01$ and ^ $p < 0.0001$ vs drug in solution. (For interpretation of the references to color in this figure legend, the reader is referred to the web version of this article.)

Nevertheless, for HES and CUR, the use of HPBCD or MBCD led to a different behavior. In the case of HPBCD, the increased apparent fluxes could be generated by the free drug and the complexed drug fractions. This reflects a possible increased drug bioavailability. Conversely, in the case of MBCD, the absence of an apparent flux is due to the strong complexation of the drugs, that leads to a much lower permeability. In fact, considering the results of phase-solubility studies and the calculated values of the binding constants ($K_{1:1}$) (Fig. 4), the drug concentration reached with MBCD was much higher, indicating a much higher hydrophilicity of the CD-drug complex.

Therefore, the permeability behavior could be related to the equilibrium constants of the CD-drug complexes as well as to their diffusivity. Indeed, both $K_{1:1}$ for RU were the lowest revealed, while for CUR, the highest constants were achieved confirming the strong complexation and the high stability of CD-CUR complexes. Moreover, the results of permeability experiments, in accordance with the diffusion coefficients of CD-CUR complexes (Table 3) obtained by UV–vis localized spectroscopy/mathematical data fitting, clarified the role of cyclodextrins as solubilizing agents in the prediction of drug bioavailability, suggesting that the drug-HPBCD complex might be less soluble but more permeable through a biomimetic barrier than the drug-MBCD one.

As it is well known, the increase of solubility is not directly related to the increase of drug diffusion and permeability (Beig et al., 2013; Morita et al., 2024). The investigational *in vitro* setting based on experimental-computational method able to discriminate the free from the bounded fraction of the selected drugs, found validation in permeability tests.

The overall results are consistent with the possibility for the CD-drug complex to permeate, especially for very stable complexes, and they shed light on the influence of complexation strategies in modifying oral absorption of lipophilic drugs, as well as the influence of UWL in permeation and diffusion mechanism.

4. Conclusions

In this work, RU, HES and CUR have been selected to investigate the formation of stable CD complexes and to demonstrate the possibility for the CD-drug complex to be absorbed and to permeate *in vivo* by using an *in vitro* experimental setup. The computational approach shed light to the conformation of CD-drug complexes as well as the strong binding responsible for the diffusion and the permeability of the drugs. We demonstrated that the newly introduced UV–vis localized spectroscopy/mathematical is a powerful tool to investigate the drug permeability mechanism of enabling formulations such as CD dispersions. Finally, we proved that the permeability of the complexes, evaluated through the state-of-the-art PermeaPad® multiwell plates, was influenced by the type of cyclodextrin utilized. The strong complexation of HES and CUR with HPBCD, with respect to MBCD, led to the formation of more permeable systems, making CD as beneficial systems for orally administered formulations. Further investigations are focused on the application of the reported *in vitro* setup on lipid-based delivery systems for RU, HES and CUR in order to compare the permeation and diffusion mechanisms in view of a targeted release.

CRediT authorship contribution statement

Maddalena Sguizzato: Writing – review & editing, Writing – original draft, Investigation, Funding acquisition, Conceptualization. **Federica Agosta:** Software, Methodology, Investigation, Formal analysis. **Antonella Ciancetta:** Writing – review & editing, Software, Methodology, Investigation, Data curation. **Mario Grassi:** Writing – review & editing, Formal analysis, Data curation. **Rita Cortesi:** Writing – review & editing, Validation, Supervision, Funding acquisition. **Massimiliano Pio di Cagno:** Writing – review & editing, Writing – original draft, Supervision, Project administration, Methodology, Data curation, Conceptualization.

Declaration of competing interest

The authors declare that they have no known competing financial interests or personal relationships that could have appeared to influence the work reported in this paper.

Acknowledgments

The research was funded by Piano Operativo Nazionale 2014–2020 Azione IV.6—Contratti di ricerca su tematiche Green (2021-PON-DM-1062- MS-RIC) and University of Ferrara (FAR 2022 and FAR 2023).

Appendix A. Supplementary data

Supplementary data to this article can be found online at https://doi.org/10.1016/j.ijpharm.2025.125170.

Data availability

Data will be made available on request.

References

Beig, A., Agbaria, R., Dahan, A., 2013. Oral delivery of lipophilic drugs: the tradeoff between solubility increase and permeability decrease when using cyclodextrin-based formulations. PLoS ONE 8, e68237. https://doi.org/10.1371/journal.pone.0068237.

Bergström, C.A.S., Charman, W.N., Porter, C.J.H., 2016. Computational prediction of formulation strategies for beyond-rule-of-5 compounds. Adv. Drug Deliv. Rev. 101, 6–21. https://doi.org/10.1016/j.addr.2016.02.005.

Berman, H.M., 2000. The protein data bank. Nucleic Acids Res. 28, 235–242. https://doi.org/10.1093/nar/28.1.235.

Carrier, R.L., Miller, L.A., Ahmed, I., 2007. The utility of cyclodextrins for enhancing oral bioavailability. J. Control. Release 123, 78–99. https://doi.org/10.1016/j.jconrel.2007.07.018.

Chang, C., Song, M., Ma, M., Song, J., Cao, F., Qin, Q., 2023. Preparation, characterization and molecular dynamics simulation of rutin–cyclodextrin inclusion complexes. Molecules 28, 955. https://doi.org/10.3390/molecules28030955.

Chua, L.S., 2013. A review on plant-based rutin extraction methods and its pharmacological activities. J. Ethnopharmacol. 150, 805–817. https://doi.org/10.1016/j.jep.2013.10.036.

Dahan, A., Miller, J.M., Amidon, G.L., 2009. Prediction of solubility and permeability class membership: provisional BCS classification of the World's top oral drugs. AAPS J 11, 740–746. https://doi.org/10.1208/s12248-009-9144-x.

Di Cagno, M., 2016. The potential of cyclodextrins as novel active pharmaceutical ingredients: a short overview. Molecules 22, 1. https://doi.org/10.3390/molecules22010001.

Di Cagno, M.P., Clarelli, F., Våbenø, J., Lesley, C., Rahman, S.D., Cauzzo, J., Franceschinis, E., Realdon, N., Stein, P.C., 2018. Experimental determination of drug diffusion coefficients in unstirred aqueous environments by temporally resolved concentration measurements. Mol. Pharmaceutics 15, 1488–1494. https://doi.org/10.1021/acs.molpharmaceut.7b01053.

Eriksen, J.B., Barakat, H., Luppi, B., Brandl, M., Bauer-Brandl, A., 2022. Modulation of paracellular-like drug transport across an artificial biomimetic barrier by osmotic stress-induced liposome shrinking. Pharmaceutics 14, 721. https://doi.org/10.3390/pharmaceutics14040721.

Gözcü, S., Polat, H.K., Gültekin, Y., Ünal, S., Karakuyu, N.F., Şafak, E.K., Doğan, O., Pezik, E., Haydar, M.K., Aytekin, E., Kurt, N., Laçin, B.B., 2024. Formulation of hesperidin-loaded *in situ* gel for ocular drug delivery: a comprehensive study. J Sci Food Agric 104, 5846–5859. https://doi.org/10.1002/jsfa.13407.

Grasso, M., Caruso, G., Godos, J., Bonaccorso, A., Carbone, C., Castellano, S., Currenti, W., Grosso, G., Musumeci, T., Caraci, F., 2021. Improving cognition with nutraceuticals targeting TGF-β1 signaling. Antioxidants 10, 1075. https://doi.org/10.3390/antiox10071075.

Haimhoffer, Á., Rusznyák, Á., Réti-Nagy, K., Vasvári, G., Váradi, J., Vecsernyés, M., Bácskay, I., Fehér, P., Ujhelyi, Z., Fenyvesi, F., 2019. Cyclodextrins in drug delivery systems and their effects on biological barriers. Sci. Pharm. 87, 33. https://doi.org/10.3390/scipharm87040033.

Hao, M., Chu, Y., Lei, J., Yao, Z., Wang, P., Chen, Z., Wang, K., Sang, X., Han, X., Wang, L., Cao, G., 2023. Pharmacological mechanisms and clinical applications of curcumin: update. Aging Dis. 14, 716. https://doi.org/10.14336/AD.2022.1101.

Higuchi, T., Connors, K.A., 1965. Phase solubility techniques: advances in analytical chemistry and instrumentation. Adv. Anal. Chem. Instrum 4, 117–212.

Holm, R., Olesen, N.E., Hartvig, R.A., Jørgensen, E.B., Larsen, D.B., Westh, P., 2016. Effect of cyclodextrin concentration on the oral bioavailability of danazol and cinnarizine in rats. Eur. J. Pharm. Biopharm. 101, 9–14. https://doi.org/10.1016/j.ejpb.2016.01.007.

Jacobsen, A.-C., Nielsen, S., Brandl, M., Bauer-Brandl, A., 2020. Drug permeability profiling using the novel permeapad® 96-well plate. Pharm Res 37, 93. https://doi.org/10.1007/s11095-020-02807-x.

Jacobsen, A.-C., Visentin, S., Butnarasu, C., Stein, P.C., Di Cagno, M.P., 2023. Commercially available cell-free permeability tests for industrial drug development: increased sustainability through reduction of in vivo studies. Pharmaceutics 15, 592. https://doi.org/10.3390/pharmaceutics15020592.

Jiang, L., Xia, N., Wang, F., Xie, C., Ye, R., Tang, H., Zhang, H., Liu, Y., 2022. Preparation and characterization of curcumin/β-cyclodextrin nanoparticles by nanoprecipitation to improve the stability and bioavailability of curcumin. LWT 171, 114149. https://doi.org/10.1016/j.lwt.2022.114149.

Kim, S., Chen, J., Cheng, T., Gindulyte, A., He, J., He, S., Li, Q., Shoemaker, B.A., Thiessen, P.A., Yu, B., Zaslavsky, L., Zhang, J., Bolton, E.E., 2023. PubChem 2023 update. Nucleic Acids Res. 51, D1373–D1380. https://doi.org/10.1093/nar/gkac956.

Li, J., Xu, F., Dai, Y., Zhang, J., Shi, Y., Lai, D., Sriboonvorakul, N., Hu, J., 2022. A Review of cyclodextrin encapsulation and intelligent response for the release of curcumin. Polymers 14, 5421. https://doi.org/10.3390/polym14245421.

Loftsson, T., Brewster, M.E., 2010. Pharmaceutical applications of cyclodextrins: basic science and product development. J. Pharm. Pharmacol. 62, 1607–1621. https://doi.org/10.1111/j.2042-7158.2010.01030.x.

Mashaqbeh, H., Obaidat, R., Al-Shar'i, N., 2021. Evaluation and characterization of curcumin-β-cyclodextrin and cyclodextrin-based nanosponge inclusion complexation. Polymers 13, 4073. https://doi.org/10.3390/polym13234073.

Molecular Operating Environment (MOE), 2022.

Morita, T., Yoshida, H., Tomita, N., Sato, Y., 2024. Comparison of in vitro screening methods for evaluating the effects of pharmaceutical excipients on membrane permeability. Int. J. Pharm. 665, 124727. https://doi.org/10.1016/j.ijpharm.2024.124727.

Morris, G.M., Huey, R., Lindstrom, W., Sanner, M.F., Belew, R.K., Goodsell, D.S., Olson, A.J., 2009. AutoDock4 and AutoDockTools4: automated docking with selective receptor flexibility. J Comput Chem 30, 2785–2791. https://doi.org/10.1002/jcc.21256.

Mukherjee, D., Krishnan, A., 2023. Therapeutic potential of curcumin and its nanoformulations for treating oral cancer. World J Methodol 13, 29–45. https://doi.org/10.5662/wjm.v13.i3.29.

Negahdari, R., Bohlouli, S., Sharifi, S., Maleki Dizaj, S., Rahbar Saadat, Y., Khezri, K., Jafari, S., Ahmadian, E., Gorbani Jahandizi, N., Raeesi, S., 2021. Therapeutic benefits of rutin and its nanoformulations. Phytother. Res. 35, 1719–1738. https://doi.org/10.1002/ptr.6904.

Paczkowska, M., Mizera, M., Piotrowska, H., Szymanowska-Powałowska, D., Lewandowska, K., Goscianska, J., Pietrzak, R., Bednarski, W., Majka, Z., Cielecka-Piontek, J., 2015. Complex of rutin with β-cyclodextrin as potential delivery system. PLoS One 10, e0120858. https://doi.org/10.1371/journal.pone.0120858.

Plaza-Garrido, M., Salinas-García, M.C., Martínez, J.C., Cámara-Artigas, A., 2020. The effect of an engineered ATCUN motif on the structure and biophysical properties of the SH3 domain of c-Src tyrosine kinase. J Biol Inorg Chem 25, 621–634. https://doi.org/10.1007/s00775-020-01785-0.

Pyrzynska, K., 2022. Hesperidin: a review on extraction methods, stability and biological activities. Nutrients 14, 2387. https://doi.org/10.3390/nu14122387.

Réti-Nagy, K., Malanga, M., Fenyvesi, É., Szente, L., Vámosi, G., Váradi, J., Bácskay, I., Fehér, P., Ujhelyi, Z., Róka, E., Vecsernyés, M., Balogh, G., Vasvári, G., Fenyvesi, F., 2015. Endocytosis of fluorescent cyclodextrins by intestinal Caco-2 cells and its role in paclitaxel drug delivery. Int. J. Pharm. 496, 509–517. https://doi.org/10.1016/j.ijpharm.2015.10.049.

Santa, K., Kumazawa, Y., Nagaoka, I., 2023. Prevention of metabolic syndrome by phytochemicals and vitamin D. IJMS 24, 2627. https://doi.org/10.3390/ijms24032627.

Saokham, P., Muankaew, C., Jansook, P., Loftsson, T., 2018. Solubility of cyclodextrins and drug/cyclodextrin complexes. Molecules 23, 1161. https://doi.org/10.3390/molecules23051161.

Schmidt, A.K., Cottaz, S., Driguez, H., Schulz, G.E., 1998. Structure of cyclodextrin glycosyltransferase complexed with a derivative of its main product β-cyclodextrin. Biochemistry 37, 5909–5915. https://doi.org/10.1021/bi9729918.

Schrödinger, L., DeLano, W., 2021. PyMOL.

Servida, S., Piontini, A., Gori, F., Tomaino, L., Moroncini, G., De Gennaro Colonna, V., La Vecchia, C., Vigna, L., 2024. Curcumin and gut microbiota: a narrative overview with focus on glycemic control. IJMS 25, 7710. https://doi.org/10.3390/ijms25147710.

Shekaari, H., Zafarani-Moattar, M.T., Mokhtarpour, M., Faraji, S., 2023. Solubility of hesperidin drug in aqueous biodegradable acidic choline chloride-based deep eutectic solvents. Sci Rep 13, 11276. https://doi.org/10.1038/s41598-023-38120-x.

Song, M., Chang, C., Wang, M., Wang, L., He, F., Wu, S., 2023. Insight into the inclusion mechanisms of curcumin in β-cyclodextrin using a screening strategy: molecular simulation and experimental study. J. Mol. Struct. 1281, 135174. https://doi.org/10.1016/j.molstruc.2023.135174.

Sugano, K., Terada, K., 2015. Rate- and extent-limiting factors of oral drug absorption: theory and applications. J. Pharm. Sci. 104, 2777–2788. https://doi.org/10.1002/jps.24391.

Tzanova, M.M., Moretti, F., Grassi, G., Stein, P.C., Hiorth, M., Abrami, M., Grassi, M., Di Cagno, M.P., 2022. Modelling drug diffusion through unstirred water layers allows real-time quantification of free/loaded drug fractions and release kinetics from colloidal-based formulations. Eur. J. Pharm. Biopharm. 178, 168–178. https://doi.org/10.1016/j.ejpb.2022.08.009.

Tzanova, M.M., Nguyen, L., Moretti, F., Grassi, M., Magnano, G.C., Voinovich, D., Stein, P.C., Hiorth, M., Di Cagno, M.P., 2023. Interpreting permeability as a function of free drug fraction: the case studies of cyclodextrins and liposomes. Eur. J. Pharm. Sci. 189, 106559. https://doi.org/10.1016/j.ejps.2023.106559.

Wahlang, B., Pawar, Y.B., Bansal, A.K., 2011. Identification of permeability-related hurdles in oral delivery of curcumin using the Caco-2 cell model. Eur. J. Pharm. Biopharm. 77, 275–282. https://doi.org/10.1016/j.ejpb.2010.12.006.

Wankar, J., Kotla, N.G., Gera, S., Rasala, S., Pandit, A., Rochev, Y.A., 2020. Recent advances in host–guest self-assembled cyclodextrin carriers: implications for responsive drug delivery and biomedical engineering. Adv Funct Materials 30, 1909049. https://doi.org/10.1002/adfm.201909049.

Wdowiak, K., Rosiak, N., Tykarska, E., Żarowski, M., Płazińska, A., Płaziński, W., Cielecka-Piontek, J., 2022. Amorphous inclusion complexes: molecular interactions of hesperidin and hesperetin with HP-B-CD and their biological effects. IJMS 23, 4000. https://doi.org/10.3390/ijms23074000.

Wei, P., Yan, X., Huang, F., 2015. Supramolecular polymers constructed by orthogonal self-assembly based on host–guest and metal–ligand interactions. Chem. Soc. Rev. 44, 815–832. https://doi.org/10.1039/C4CS00327F.

Xiong, H., Wang, J., Ran, Q., Lou, G., Peng, C., Gan, Q., Hu, J., Sun, J., Yao, R., Huang, Q., 2019. Hesperidin: a therapeutic agent for obesity. DDDT 13, 3855–3866. https://doi.org/10.2147/DDDT.S227499.

Yadav, V.R., Suresh, S., Devi, K., Yadav, S., 2009. Effect of cyclodextrin complexation of curcumin on its solubility and antiangiogenic and anti-inflammatory activity in rat colitis model. AAPS PharmSciTech 10, 752. https://doi.org/10.1208/s12249-009-9264-8.

Yusuf, H., Meidy Nurintan Savitri, O., Primaharinastiti, R., Agus Syamsur Rijal, M., 2023. A lyophilized surfactant-based rutin formulation with improved physical characteristics and dissolution for oral delivery. Saudi Pharmaceutical Journal 31, 1077–1083. https://doi.org/10.1016/j.jsps.2023.03.018.